


Article

Flexible n-Type Tungsten Carbide/Polylactic Acid Thermoelectric Composites Fabricated by Additive Manufacturing

Yong Du ^{1,2,*} , Jiageng Chen ¹, Xin Liu ¹, Chun Lu ³, Jiayue Xu ¹, Biplab Paul ² and Per Eklund ^{2,*}

¹ School of Materials Science and Engineering, Shanghai Institute of Technology, Shanghai 201418, China; 176081125@mail.sit.edu.cn (J.C.); 166081114@mail.sit.edu.cn (X.L.); xujiayue@sit.edu.cn (J.X.)

² Thin Film Physics Division, Department of Physics, Chemistry, and Biology (IFM), Linköping University, SE-58183 Linköping, Sweden; biplab.paul@liu.se

³ College of Aerospace Engineering, Shenyang Aerospace University, Shenyang 110136, China; luchun1024@126.com

* Correspondence: ydu@sit.edu.cn or yong.du@liu.se (Y.D.); per.eklund@liu.se (P.E.)

Received: 14 October 2017; Accepted: 13 November 2017; Published: 4 January 2018

Abstract: Flexible n-type tungsten carbide/polylactic acid (WC/PLA) composites were fabricated by additive manufacturing and their thermoelectric properties were investigated. The preparation of an n-type polymer-based thermoelectric composite with good stability in air atmosphere via additive manufacturing holds promise for application in flexible thermoelectric devices. For WC/PLA volume ratios varying from ~33% to 60%, the electrical conductivity of the composites increased from 10.6 to 42.2 S/cm, while the Seebeck coefficients were in the range -11 to -12.3 $\mu\text{V/K}$. The thermal conductivities of the composites varied from ~ 0.2 to ~ 0.28 $\text{W}\cdot\text{m}^{-1}\cdot\text{K}^{-1}$ at ~ 300 K.

Keywords: flexible thermoelectrics; additive manufacturing; tungsten carbide; polylactic acid; composites

1. Introduction

Thermoelectric (TE) power generators or refrigerators are based on the Seebeck effect or Peltier effect, respectively, and have the ability to convert heat into electrical power and vice versa. They also have high reliability, do not require maintenance, and are environmentally friendly [1]. The efficiency of TE devices depends on the dimensionless figure of merit, $ZT = S^2\sigma T/\kappa$ (where S is the Seebeck coefficient, σ is the electrical conductivity, T is the absolute temperature, and κ is the thermal conductivity) [2].

Polymers typically have about one order of magnitude lower thermal conductivity than traditional inorganic TE materials, e.g., Bi–Te-, Ge–Si-, and Pb–Te-based alloys [3]. Furthermore, polymers have low density, cost little, and are easy to fabricate [4], and are interesting for thermoelectrics in themselves [5–8], but are also suitable matrices for fabrication of inorganic-polymer TE composites. Both conducting and non-conducting polymers have been used for TE materials. Attention has also been paid to polymer-based TE composites, such as Te/poly(3,4-ethylenedioxythiophene):poly(styrenesulfonate) (PEDOT:PSS) [9], Bi₂Te₃/PEDOT:PSS [10], SnSe/PEDOT:PSS [11], carbon nanotube/poly(vinyl acetate) [12], and single-walled carbon nanotubes/polyaniline [13]. Using traditional methods, e.g., physical mixing [14], solution mixing [15], and in situ polymerization [16,17], the preparation of polymer-based TE composites tends to cause oxidation and uneven dispersion in the polymer matrices [3], which influences the TE properties of the polymer-based composites. The TE properties of polymers and polymer-based TE composites have been greatly enhanced [9–11], with ZT values up to 0.42 having been achieved [18]. However, these polymer-based TE materials

and composites are mainly p-type. n-type polymer-based TE composites have issues with stability in air [19], because reduced polymer chains and counteractions (e.g., alkaline metal ions) are easily oxidized [20], resulting in instability in the atmospheric environment [21]. Fabricating TE devices require both p-type and n-type materials, placing a severe restriction on the application of polymer-based composites in TE devices [22]. Therefore, it is important to develop a new approach for fabricating n-type polymer-based TE composites.

Additive manufacturing (3D printing), first described by Hull in 1986 [23], has revolutionized materials technology, yielding large savings in both materials and time, and an ability to design complex geometric configurations [24]. However, few researchers have used additive manufacturing for TE materials. He et al. [25] fabricated $\text{Bi}_{0.5}\text{Sb}_{1.5}\text{Te}_3$ alloys via stereolithography additive manufacturing combined with thermal annealing at 350 °C under Ar gas to remove photoresins. Most recently, Shishkovsky et al. [26] prepared porous gradient polymer nanocomposite materials consisting of a polyetheretherketone matrix doped with alternating layers of Ni and Cu nanoparticles via selective laser sintering additive manufacturing. To some extent, additive manufacturing may be an alternative to hot-pressing and spark plasma sintering methods for the preparation of inorganic TE materials [25]. However, it is a challenge to prepare conducting polymer-based TE composites using additive manufacturing, since most conducting polymers are infusible and insoluble because of the presence of the extended conjugation along the polymer backbone [27,28]. Compared to conducting polymers, polylactic acid (PLA) have better processability [29], which is suitable for additive manufacturing. However, no research on the preparation and TE properties of PLA-based composites has been reported.

In this work, flexible n-type tungsten carbide/polylactic acid (WC/PLA) TE composites were prepared by additive manufacturing, which holds promise for application in flexible TE devices. The influence of WC content on the morphology and TE properties of WC/PLA composites is investigated.

2. Materials and Methods

2.1. Materials

Tungsten carbide (WC, 200 mesh) and chloroform were purchased from Sinopharm Chemical Reagent Co., Ltd. (Shanghai, China). PLA (1.75 mm 3D filament) was obtained from Shenyang Gein Technology Co., Ltd. (Shenyang, China). All the materials were used without further treatment or purification.

2.2. Preparation of n-Type WC/PLA Composites

Exactly 0.8 g of PLA was dissolved in 12 mL of chloroform (Solution I). An appropriate amount of WC (to obtain WC/PLA mass ratios of 5:0.8, 10:0.8, 15:0.8, and 20:0.8, corresponding to nominal volume ratios of ~33%, 50%, 60%, and 67%, respectively) was added to Solution I and stirred for 2 h to produce Solution II. Solution II was inhaled in the 10 mL syringes and then printed using a 3D solution printer (Shenzhen Polymer Science & Technology Ltd., Model: PLM-I, Shenzhen, China) with a nozzle diameter of 0.5 mm and a print speed of 300 mm/min (fixed parameter). After being dried at 60 °C for 12 h, the chloroform was evaporated from the mixed solution, and the WC/PLA composites were then formed. Figure 1a shows the 3D fabrication process of the WC/PLA composites. The WC/PLA composites with the WC/PLA mass ratios of 5:0.8, 10:0.8, 15:0.8, and 20:0.8 (corresponding to nominal volume ratios of ~33%, 50%, 60%, and 67%, respectively) are denoted as WP5, WP10, WP15, and WP20, respectively.

2.3. Characterization

The samples were characterized using scanning electron microscopy (SEM) (Philips XL 30 FEG, Eindhoven, The Netherlands) and X-ray diffraction (XRD) (Bruker D8 Advance, Karlsruhe,

Germany), respectively. Seebeck coefficients and electrical conductivities of the WC/PLA composites were measured simultaneously in an MRS-3L thin-film thermoelectric test system in a low-vacuum atmosphere (≤ 40 Pa) from 150 to 375 K with instrument test errors of 6% and 5% for the Seebeck coefficient and electrical conductivity, respectively (Wuhan Giant Instrument Technology Co., Ltd., Wuhan, China). Thermal conductivities of the samples were measured by a transient hot-wire method from 300 to 375 K with a TC3000E thermal conductivity meter (Xiotech Electronics Co., Ltd., Xi'an, China), and three measurements were performed for each sample. The average value is reported.

3. Results and Discussion

Figure 1b shows an SEM image of the as-received WC particles. The size of WC particles is in the range of ~ 1 to ~ 5 μm , and the WC particles are aggregated together. Figure 1c shows XRD patterns of WC/PLA composites with different amounts of WC. All peaks in Figure 1c can be indexed to WC (JCPDF, No. 51-0939), mainly because of the amorphous character of PLA. There is no change in the position of the diffraction peaks with the addition of WC to the PLA matrix, which indicates that no other phase was formed. EDS analysis showed that the material contains C, O, and W, as expected. Figure 1d shows the flexibility of the sample WP5, which can be easily bent in an almost fully reversible manner.

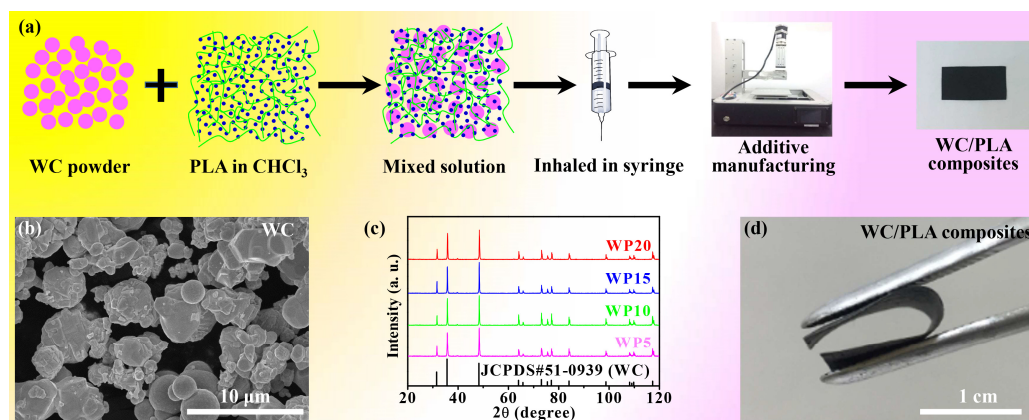


Figure 1. Schematic of the fabrication process of the WC/PLA thermoelectric composites (a), SEM image of tungsten carbide (WC) (b), XRD patterns of tungsten carbide/poly(lactic acid) (WC/PLA) composites with different WC loadings (c), and the flexible display digital photo of the WP5 (d).

Figure 2a–h show SEM surface images of the WC/PLA composites with different amounts of WC. The WC particles have been well dispersed in the PLA matrices. Figure 2i,j show the SEM images of a fracture surface of the WP20 composite. The thickness measured in Figure 2i is ~ 170 μm . Figure 2k,l show SEM-EDS maps of the fracture cross-section and the top-view surface of the WP20 composite, respectively. W is evenly distributed in the EDS maps of both the fracture cross-section and the top-view surface of the composites, which indicates that WC is evenly distributed in the PLA matrices.

The electrical conductivity, Seebeck coefficient, power factor ($S^2\sigma$), thermal conductivity, and ZT of the WC/PLA composites with different amounts of WC are shown in Figure 3. Note that the volume fraction of WC in the sample WP20 is 67%. As a result, this sample is not as flexible as the others. For this reason, only the TE properties of samples WP5, WP10, and WP15 are reported here. The electrical conductivity of all the composites decreases with increasing temperature from 150 to 375 K. For increasing WC content (WP5, WP10, and WP15), the electrical conductivity increased from 16.7 to 51.1 S/cm at ~ 150 K, mainly because WC has a relatively high electrical conductivity. This conductivity is much higher than that of most reported n-type conducting polymers and corresponding composites, such as the conjugated polymer ClBDPPV combined with 25 mol % tetrabutylammonium fluoride (0.62 S/cm) [30], the α -1-ethyl-3-methylimidazolium

ethyl-sulfate-doped polyaniline (0.23 S/cm) [31], the poly[$K_x(\text{Ni-ett})$] blended with poly(vinylidene fluoride) (PVDF)/DMSO on paper (0.5 S/cm) [32]. However, this value is smaller than that of Ni nanowire/PVDF nanocomposites (4701 S/cm), due to the much higher electrical conductivity of Ni nanowires (2.98×10^4 S/cm) [33].

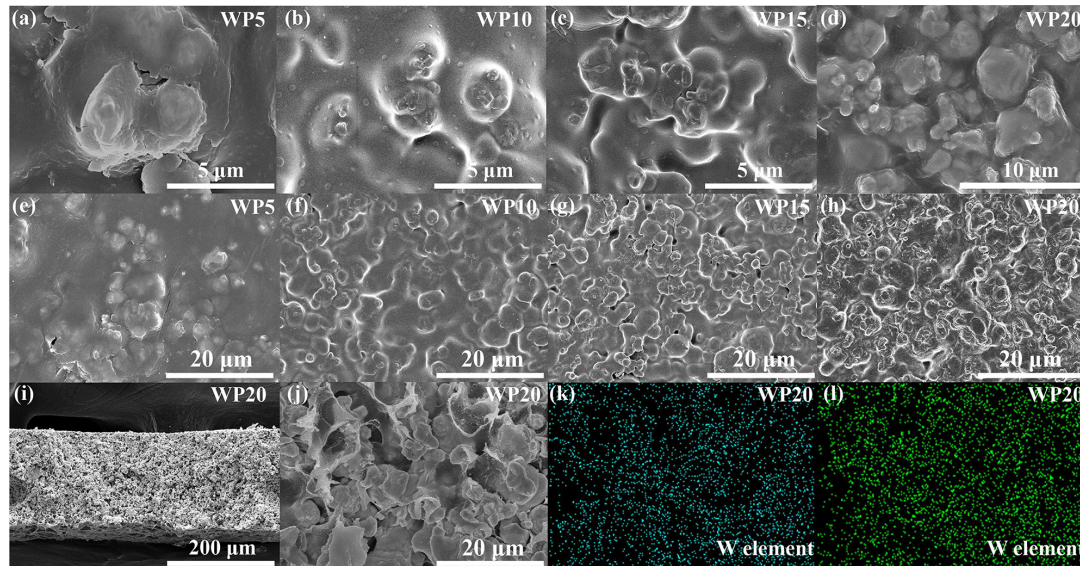


Figure 2. SEM images of WP5 (a,e), WP10 (b,f), WP15 (c,g), and WP20 (d,h), fracture surface of WP20 (i,j). (k,l) are the corresponding SEM-EDS mapping (W element) images of the panel (j,d), respectively.

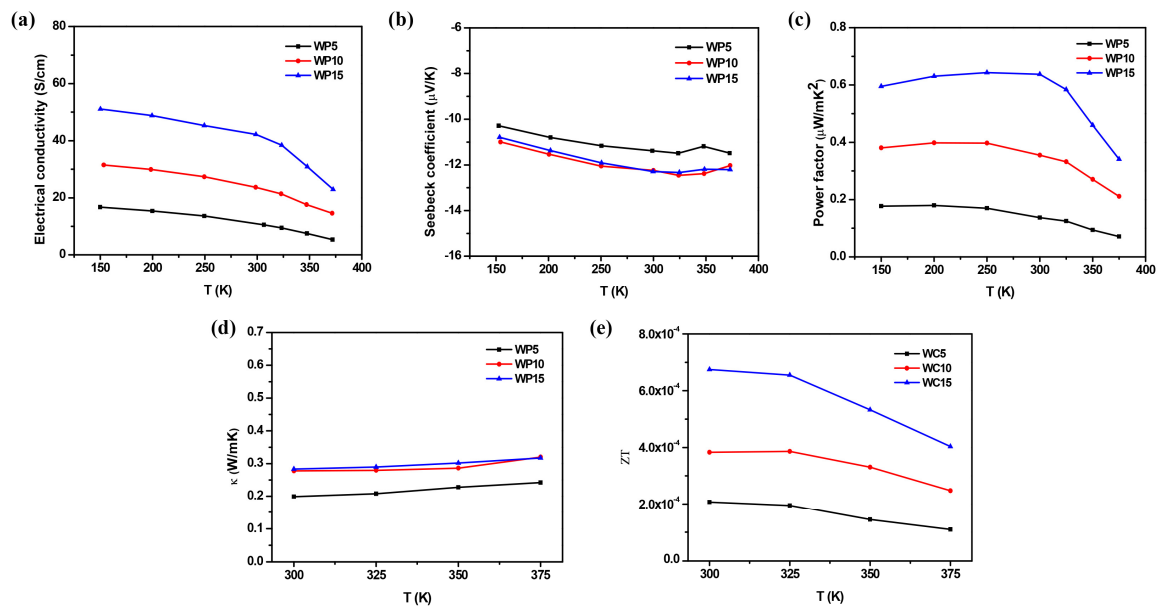


Figure 3. Electrical conductivity (a), Seebeck coefficient (b), calculated power factor (c), thermal conductivity (d), and ZT (e) of the WC/PLA thermoelectric composites.

The Seebeck coefficients of all the composites are negative, indicating n-type conduction. The Seebeck coefficients of all composites are almost the same (between -10.3 and -12.5 $\mu\text{V/K}$) in the measured temperature range from 150 to 375 K. The power factor follows essentially the same trend as the electrical conductivity, given that the variations in the Seebeck coefficient are rather small.

The electrical conductivity and Seebeck coefficient of the composites remained unchanged after storage in air for one month, showing the long-term stability of the composites.

A maximum power factor of $0.64 \mu\text{W}\cdot\text{m}^{-1}\cdot\text{K}^{-2}$ at 250 K was obtained from sample WP15. This is a low value compared to inorganic materials (typically ranging from $\sim 1 \times 10^{-4}$ to $\sim 4 \times 10^{-3} \text{W}\cdot\text{m}^{-1}\cdot\text{K}^{-2}$) [34,35] or the best organic thermoelectrics ($\sim 100\text{--}500 \mu\text{W}\cdot\text{m}^{-1}\cdot\text{K}^{-2}$) [18], but still higher than, for example, that of the conjugated polymer ClBDPPV combined with 25 mol % tetrabutylammonium fluoride ($0.63 \mu\text{W}\cdot\text{m}^{-1}\cdot\text{K}^{-2}$) [30], 1-ethyl-3-methylimidazolium ethyl-sulfate-doped polyaniline ($4.43 \times 10^{-3} \mu\text{W}\cdot\text{m}^{-1}\cdot\text{K}^{-2}$) [31], or poly[K_x(Ni-ett)] blended with poly(vinylidene fluoride) (PVDF)/DMSO on paper ($4.1 \times 10^{-2} \mu\text{W}\cdot\text{m}^{-1}\cdot\text{K}^{-2}$) [32].

The thermal conductivities of the composites were measured three times at different temperatures and the average values are reported in Figure 3d. The thermal conductivities at 300 K of the WC/PLA composites vary from ~ 0.20 to $\sim 0.28 \text{W}\cdot\text{m}^{-1}\cdot\text{K}^{-1}$, which are slightly higher than that of the PLA ($\sim 0.13 \text{W}\cdot\text{m}^{-1}\cdot\text{K}^{-1}$ [36]), but two orders of magnitudes lower than that of WC ($29\text{--}121 \text{W}\cdot\text{m}^{-1}\cdot\text{K}^{-1}$ [37]), mainly because the surface of WC particles are coated by PLA (Figure 2a–h). The thermal conductivities for all the samples increase slowly as temperatures increase from 300 to 375 K. Figure 4d shows the corresponding ZT values of the samples. As the WC content increases, the electrical conductivities of the composites increase, while the Seebeck coefficients and thermal conductivities of the composites are not very sensitive; as a result, the ZT value of the composites increase, and the highest ZT value of $\sim 6.7 \times 10^{-4}$ at 300 K is obtained for WP15. The average value of the three measurements of electrical resistance for WP5 increased by 6.6% after being bent 300 times at different bending radii (100 times at bending radii of 13 mm, 100 mm, and 8.1 mm, respectively), while the Seebeck coefficient almost remain unchanged, which indicates that WP5 has good flexibility (Figure 1d). However, the increase in WC in composite material deteriorated its flexibility. This is a relatively low ZT as a consequence of the modest power factor. However, the purpose of the present work was to demonstrate a stable n-type polymer/inorganic composite for thermoelectrics. To increase the ZT value, different inorganic fillers can be used. Furthermore, the additive manufacturing process used in this work has many advantages, as it is, e.g., convenient, cost-effective, maneuverable, and scalable. This preparation route can print a wide range of desired shapes of WC/PLA composites (illustrated in Figure 4). This versatility combined with the fact that the as-prepared WC/PLA composites are stable in air suggests that the methodology can be extended to other polymer-based TE composites.

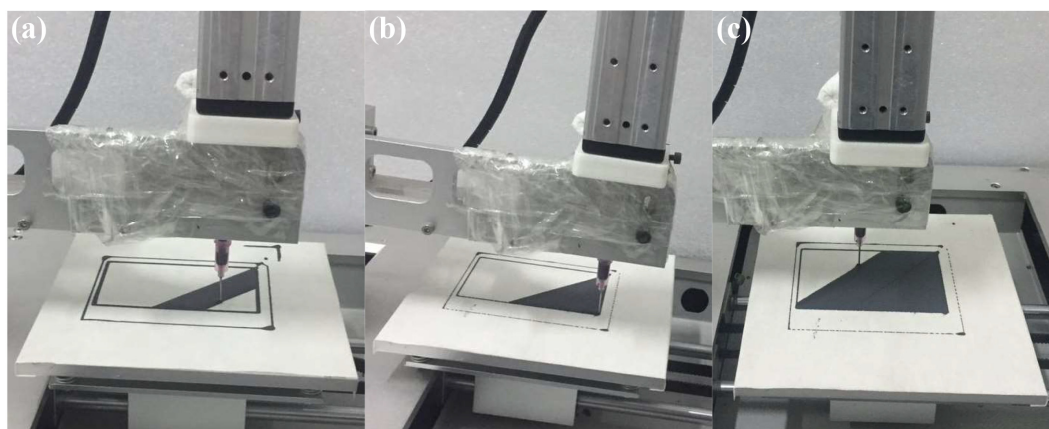


Figure 4. Photograph of the additive manufacturing process, showing the variation in shape of the synthesized materials.

4. Conclusions

Flexible, n-type tungsten carbide/polylactic acid (WC/PLA) thermoelectric composites were prepared by additive manufacturing. The highest ZT value ($\sim 6.7 \times 10^{-4}$ at 300 K) of the WC/PLA

thermoelectric composites (the mass ratio of WC/PLA is 15:0.8) was achieved. This is the first time n-type polymer-based composites prepared via additive manufacturing have been reported. This process can print almost any designed shape of polymer-based thermoelectric composites, and the as-prepared n-type polymer-based thermoelectric composites have good flexibility and stability, and thus have great potential for flexible thermoelectric devices.

Acknowledgments: This work has been supported by the National Natural Science Foundation of China (61611530550, 61504081), the Program for Professor of Special Appointment (Young Eastern Scholar Program) at Shanghai Institutions of Higher Learning (QD2015039), and the Shanghai Innovation action plan project (17090503600). We also acknowledge support from the European Research Council under the European Community's Seventh Framework Programme (FP/2007-2013)/ERC grant agreement No. 335383, the Swedish Research Council (VR) under project No. 2016-3365, the Eurostars project E!8892 T-to-Power, and the Swedish Foundation for Strategic Research (SSF) through the Future Research Leaders 5 program.

Author Contributions: Yong Du designed the experiments, data analysis, and wrote the manuscript. Jiageng Chen, Xin Liu, Chun Lu, and Jiayue Xu helped perform the experiments and data analysis. Biplab Paul and Per Eklund contributed to discussion and interpretations and revised the manuscript.

Conflicts of Interest: The authors declare no conflict of interest.

References

1. Snyder, G.J.; Toberer, E.S. Complex thermoelectric materials. *Nat. Mater.* **2008**, *7*, 105–114. [[CrossRef](#)] [[PubMed](#)]
2. Majumdar, A. Thermoelectricity in semiconductor nanostructures. *Science* **2004**, *303*, 777–778. [[CrossRef](#)] [[PubMed](#)]
3. Du, Y.; Shen, S.Z.; Cai, K.F.; Casey, P.S. Research progress on polymer-inorganic thermoelectric nanocomposite materials. *Prog. Polym. Sci.* **2012**, *37*, 820–841. [[CrossRef](#)]
4. Bahk, J.H.; Fang, H.Y.; Yazawa, K.; Shakouri, A. Flexible thermoelectric materials and device optimization for wearable energy harvesting. *J. Mater. Chem. C* **2015**, *3*, 10362–10374. [[CrossRef](#)]
5. Bubnova, O.; Khan, Z.U.; Malti, A.; Braun, S.; Fahlman, M.; Berggren, M.; Crispin, X. Optimization of the thermoelectric figure of merit in the conducting polymer poly(3,4-ethylenedioxythiophene). *Nat. Mater.* **2011**, *10*, 429–433. [[CrossRef](#)] [[PubMed](#)]
6. Bubnova, O.; Khan, Z.U.; Wang, H.; Braun, S.; Evans, D.R.; Fabretto, M.; Hojati-Talemi, P.; Dagnelund, D.; Arlin, J.B.; Geerts, Y.H. Semi-metallic polymers. *Nat. Mater.* **2014**, *13*, 190–194. [[CrossRef](#)] [[PubMed](#)]
7. Bubnova, O.; Crispin, X. Towards polymer-based organic thermoelectric generators. *Energy Environ. Sci.* **2012**, *5*, 9345–9362. [[CrossRef](#)]
8. He, M.; Qiu, F.; Lin, Z. Towards high-performance polymer-based thermoelectric materials. *Energy Environ. Sci.* **2013**, *6*, 1352–1361. [[CrossRef](#)]
9. See, K.C.; Feser, J.P.; Chen, C.E.; Majumdar, A.; Urban, J.J.; Segalman, R.A. Water-processable polymer-nanocrystal hybrids for thermoelectrics. *Nano Lett.* **2010**, *10*, 4664–4667. [[CrossRef](#)] [[PubMed](#)]
10. Du, Y.; Cai, K.F.; Chen, S.; Cizek, P.; Lin, T. Facile preparation and thermoelectric properties of Bi₂Te₃ based alloy nanosheet/PEDOT:PSS composite films. *ACS Appl. Mater. Interfaces* **2014**, *6*, 5735–5743. [[CrossRef](#)] [[PubMed](#)]
11. Ju, H.; Kim, J. Chemically exfoliated SnSe nanosheets and their SnSe/poly(3,4-ethylenedioxythiophene):poly(styrenesulfonate) composite films for polymer based thermoelectric applications. *ACS Nano* **2016**, *10*, 5730–5739. [[CrossRef](#)] [[PubMed](#)]
12. Yu, C.; Kim, Y.S.; Kim, D.; Grunlan, J.C. Thermoelectric behavior of segregated-network polymer nanocomposites. *Nano Lett.* **2008**, *8*, 4428–4432. [[CrossRef](#)] [[PubMed](#)]
13. Yao, Q.; Chen, L.; Zhang, W.; Liufu, S.; Chen, X. Enhanced thermoelectric performance of single-walled carbon nanotubes/polyaniline hybrid nanocomposites. *ACS Nano* **2010**, *4*, 2445–2451. [[CrossRef](#)] [[PubMed](#)]
14. Zhao, X.B.; Hu, S.H.; Zhao, M.J.; Zhu, T.J. Thermoelectric properties of Bi_{0.5}Sb_{1.5}Te₃/polyaniline hybrids prepared by mechanical blending. *Mater. Lett.* **2002**, *52*, 147–149. [[CrossRef](#)]
15. Toshima, N.; Imai, M.; Ichikawa, S. Organic-inorganic nanohybrids as novel thermoelectric materials: Hybrids of polyaniline and bismuth(iii) telluride nanoparticles. *J. Electron. Mater.* **2011**, *40*, 898–902. [[CrossRef](#)]

16. Du, Y.; Cai, K.F.; Shen, S.Z.; Casey, P.S. Preparation and characterization of graphene nanosheets/poly (3-hexylthiophene) thermoelectric composite materials. *Synth. Met.* **2012**, *162*, 2102–2106. [\[CrossRef\]](#)
17. Wang, Y.Y.; Cai, K.F.; Yin, J.L.; An, B.J.; Du, Y.; Yao, X. In situ fabrication and thermoelectric properties of PbTe-polyaniline composite nanostructures. *J. Nanopart. Res.* **2011**, *13*, 533–539. [\[CrossRef\]](#)
18. Kim, G.H.; Shao, L.; Zhang, K.; Pipe, K.P. Engineered doping of organic semiconductors for enhanced thermoelectric efficiency. *Nat. Mater.* **2013**, *12*, 719–723. [\[CrossRef\]](#) [\[PubMed\]](#)
19. Wei, Q.S.; Mukaida, M.; Kirihaara, K.; Naitoh, Y.; Ishida, T. Polymer thermoelectric modules screen-printed on paper. *RSC Adv.* **2014**, *4*, 28802–28806. [\[CrossRef\]](#)
20. Yamaguchi, I.; Mitsuno, H. Synthesis of n-type π -conjugated polymers with pendant crown ether and their stability of n-doping state against air. *Macromolecules* **2010**, *43*, 9348–9354. [\[CrossRef\]](#)
21. Stepien, L.; Roch, A.; Tkachov, R.; Gedrange, T. Progress in polymer thermoelectrics. In *Thermoelectrics for Power Generation-A Look at Trends in the Technology*; Skipidarov, S., Nikitin, M., Eds.; InTech: Rijeka, Croatia, 2016; pp. 147–161.
22. Wang, S.; Sun, H.; Ail, U.; Vagin, M.; Persson, P.O.Å.; Andreasen, J.W.; Thiel, W.; Berggren, M.; Crispin, X.; Fazzi, D.; et al. Thermoelectric properties of solution-processed n-doped ladder-type conducting polymers. *Adv. Mater.* **2016**, *28*, 10764–10771. [\[CrossRef\]](#) [\[PubMed\]](#)
23. Hull, C.W. Apparatus for Production of three-Dimensional Objects by Stereolithography. U.S. Patent 4,575,330, 11 March 1986.
24. Bhushan, B.; Caspers, M. An overview of additive manufacturing (3D printing) for microfabrication. *Microsyst. Technol.* **2017**, *23*, 1117–1124. [\[CrossRef\]](#)
25. He, M.; Zhao, Y.; Wang, B.; Xi, Q.; Zhou, J.; Liang, Z. 3D printing: 3D printing fabrication of amorphous thermoelectric materials with ultralow thermal conductivity. *Small* **2015**, *11*, 5889–5894. [\[CrossRef\]](#) [\[PubMed\]](#)
26. Shishkovsky, I.; Scherbakov, V.; Saraeva, I.; Ionin, A. Thermoelectric properties of gradient polymer composites with nano-inclusions fabricated by laser assisted sintering. *Laser Phys. Lett.* **2017**, *14*, 035601. [\[CrossRef\]](#)
27. Wen, Y.; Xu, J. Scientific importance of water-processable PEDOT-PSS and preparation, challenge and new application in sensors of its film electrode: A review. *J. Polym. Sci. Part A Polym. Chem.* **2017**, *55*, 1121–1150. [\[CrossRef\]](#)
28. Ramakrishnan, S. From a laboratory curiosity to the market place. *Resonance* **2011**, *16*, 1254–1265. [\[CrossRef\]](#)
29. Rasal, R.M.; Janorkar, A.V.; Hirt, D.E. Poly(lactic acid) modifications. *Prog. Polym. Sci.* **2010**, *35*, 338–356. [\[CrossRef\]](#)
30. Zhao, X.G.; Madan, D.; Cheng, Y.; Zhou, J.W.; Li, H.; Thon, S.M.; Bragg, A.E.; DeCoster, M.E.; Hopkins, P.E.; Katz, H.E. High conductivity and electron-transfer validation in an n-type fluoride-anion-doped polymer for thermoelectrics in air. *Adv. Mater.* **2017**, *29*, 1606928. [\[CrossRef\]](#) [\[PubMed\]](#)
31. Yoo, D.; Lee, J.J.; Park, C.; Choi, H.H.; Kim, J.H. N-type organic thermoelectric materials based on polyaniline doped with the aprotic ionic liquid 1-ethyl-3-methylimidazolium ethyl sulfate. *RSC Adv.* **2016**, *6*, 37130–37135. [\[CrossRef\]](#)
32. Menon, A.K.; Meek, O.; Eng, A.J.; Yee, S.K. Radial thermoelectric generator fabricated from n- and p-type conducting polymers. *J. Appl. Polym. Sci.* **2017**, *134*, 44060. [\[CrossRef\]](#)
33. Chen, Y.N.; He, M.H.; Liu, B.; Bazan, G.C.; Zhou, J.; Liang, Z.Q. Bendable n-type metallic nanocomposites with large thermoelectric power factor. *Adv. Mater.* **2017**, *29*, 1604752. [\[CrossRef\]](#) [\[PubMed\]](#)
34. Paul, B.; Lu, J.; Eklund, P. Nanostructural tailoring to induce flexibility in thermoelectric $\text{Ca}_3\text{Co}_4\text{O}_9$ thin films. *ACS Appl. Mater. Interfaces* **2017**, *9*, 25308–25316. [\[CrossRef\]](#) [\[PubMed\]](#)
35. Zhao, L.D.; Lo, S.H.; Zhang, Y.S.; Sun, H.; Tan, G.J.; Uher, C.; Wolverton, C.; Dravid, V.P.; Kanatzidis, M.G. Ultralow thermal conductivity and high thermoelectric figure of merit in SnSe crystals. *Nature* **2014**, *508*, 373–377. [\[CrossRef\]](#) [\[PubMed\]](#)
36. Hassouna, F.; Laachachi, A.; Chapron, D.; El Mouedden, Y.; Toniazzi, V.; Ruch, D. Development of new approach based on Raman spectroscopy to study the dispersion of expanded graphite in poly(lactide). *Polym. Degrad. Stab.* **2011**, *96*, 2040–2047. [\[CrossRef\]](#)
37. Abyzov, A.M.; Kidalov, S.V.; Shakhov, F.M. High thermal conductivity composites consisting of diamond filler with tungsten coating and copper (silver) matrix. *J. Mater. Sci.* **2011**, *46*, 1424–1438. [\[CrossRef\]](#)

